

Laser and Microwave Generations in Nitrogen

Mladen M. Kekez 

Abstract—This paper describes the results obtained in the three sets of experiments. The laser emission and microwaves have been obtained almost with the same experimental setup. The ultraviolet radiation coming from the current carrying the spark channel pumps the N₂ molecules to the upper-excited $C^3\pi_u$ level to yield the nitrogen laser pulses at 337.1 nm of long (>220 ns) duration in the experimental setup used. The electromagnetic waves observed at the single microwave frequency close to 1 GHz and at 337.1 nm (=prominent nitrogen laser line) are the coherent radiations due to the maser action and the laser action, respectively. An attempt is made to relate one of these concepts to the lightning phenomena.

Index Terms—High-power microwaves, lightning, nitrogen laser, spark and corona discharges.

I. INTRODUCTION

MOLECULES have a large and varied family of vibrational modes. Each mode has its own precise excitation energy, and all the adjacent levels of a given mode are separated by that amount of energy. To obtain the lasing action, the vibrational transitions have been studied in detail. It is now accepted that the lasers can be made to work in the wide range of the wavelengths, λ ranging over three decades ($\lambda = 100 \mu\text{m}$ to 100 nm, i.e., frequency $f = 3 \times 10^{12}$ to 3×10^{15} Hz) and covering the infrared domain, the visible spectra and the ultraviolet (UV) domain [1].

The atomic hydrogen maser [2] is also the source of the coherent radiation, but this is due to the maser action (=microwave amplification by stimulated emission of radiation). It uses the intrinsic properties of the hydrogen atom. The amount of energy needed to reverse the spin of the hydrogen electron is equivalent to a photon at a frequency of 1.420 GHz. This corresponds to the atomic transition between the two hyperfine levels of the hydrogen atom, and an energy difference of $5.87433 \mu\text{eV}$. The atomic hydrogen maser serves as a precision frequency reference to get the atomic hydrogen clock [3]. The resonant cavity of the hydrogen maser is tuned to a precise frequency of 1.420 GHz.

There are dozens of rotational levels associated with each vibrational level. The rules of quantum mechanics require that a molecule changes exactly one rotational level when it moves from one vibrational level to another. The result is that each vibrational transition includes many possible rotational

transitions. The overall net effect is that the vibrational lasers emit a broad range of wavelengths. The N₂ laser is a good example of how this lasing action works (=light amplification by stimulated emission of radiation).

The N₂ laser radiates mainly at about ten different spectral lines. The prominent radiation line of the radiation band of the N₂ molecules occurs in the UV domain at 337.1 nm ($f = 8.899 \times 10^{14}$ Hz and photon energy = 3.68 eV). With the transverse excitation method using the Blumlein transmission line circuit [4]–[6], the radiation takes the form of short pulses. The high gain leads to relatively efficient superluminescent emissions even without a laser resonator. However, the addition of a rear mirror boosts the power over 2.5 times.

The large fraction of the overall emission comes from the second positive band of N₂. The population states of the nitrogen molecule are determined according to the Franck–Condon principle.

The main consideration in the design of the N₂ lasers is that the pumping rate should be faster than the lifetime of the upper-excited level, so that an inversion of the population can be attained before the spontaneous emissions decay. The only way to get the laser action to occur is to populate rapidly the upper-excited level.

At low (few torr) pressure of N₂, the lifetime of the upper-excited $C^3\pi_u$ level (at about 10 eV) of the N₂ molecules is about 40 ns. This is much shorter than that of the lower excited (metastable) $B^3\pi_g$ level (at about 6.3 eV) which can last for a long time (up to many milliseconds).

At higher pressure, the lifetime of the upper level becomes even shorter consequently, and it becomes harder to establish the inversion threshold. Excitation of the N₂ molecules at close to atmospheric pressure yields short-duration light pulses from 1 ns down to some tens of picoseconds.

The data above stated are related to the condition when the Blumlein transmission line circuit is used. Under this condition, the laser pumping to upper-excited $C^3\pi_u$ level is achieved by the application of the electrical field that is rapidly falling in time. This fall of the electric field value versus time increases as the pressure rises.

The purpose of this paper is to demonstrate experimentally that the microwave (maser) generation, and the laser radiation can be produced simultaneously almost with the same experimental setup. Because the N₂ laser does not require the mirrors in the resonator, nitrogen was used to be the lasing (gain) medium in the experiments.

The classical method of N₂ laser production is to use the Blumlein circuit to get the glow-like column to be the gain medium. This method makes the pumping to the upper-excited $C^3\pi_u$ level to be done in a short period of time. In contrast to this approach, a new method is suggested in this paper.

Manuscript received October 11, 2017; revised January 5, 2018; accepted January 18, 2018. The review of this paper was arranged by Senior Editor D. A. Shiffler and language editing was done by Senior English Editor M. Rafferty.

The author is with High-Energy Frequency Tesla Inc., Ottawa, ON K1H 7L8, Canada (e-mail: mkekez@magma.ca).

Color versions of one or more of the figures in this paper are available online at <http://ieeexplore.ieee.org>.

Digital Object Identifier 10.1109/TPS.2018.2796304

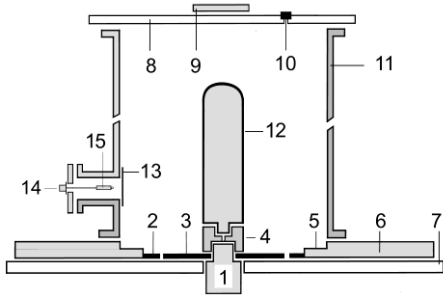


Fig. 1. Schematic of the experimental setup. 1—HV terminal connected to the Marx generator, 2—copper ring, 3—copper plate, 4—metallic holder connected to the generator, 5—step in the metallic flange, 6—metallic flange connected to the enclosure of the generator, 7 and 8—Plexiglas flanges, 9—partial reflector, 10—337-nm bandpass filter, 11—cylinder of 6-in (=15.24-cm) diameter, 12—graphite electrode of 2-in (=5.08-cm) diameter, 13—copper mesh, 14—BNC connector, and 15—Tektronix CT-1 probe placed into 2 $\frac{3}{4}$ inches nipple. B-dot probe was placed above the partial reflector, and the photodiode was placed above 337-nm bandpass filter.

It involves the UV radiation to pump the N_2 molecules to the upper-excited $C^3\pi_u$ level for a long time. As the consequence, the new method yields the N_2 laser pulses of long (>220 ns) duration. To demonstrate this idea, three sets of experiments have been performed. In the first set of experiments, the classical method was used to produce the N_2 laser radiation at 337.1 nm. In the second set of experiments, the electrical pulse from nine-stage Marx generator was applied to the structure given in Fig. 1. The microwave emissions close to 1 GHz have been obtained. These microwave data are in accordance with the data presented earlier [7]–[9]. In the third set of experiments, it was insured that the current carrying the spark channel under observation will conduct a large portion of the total current flowing in the setup. This makes that the spark channel will keep producing the UV radiation. In turn, the UV radiation will also keep pumping the upper-excited $C^3\pi_u$ level of the N_2 molecules yielding the laser pulses at 337.1 nm of long (>220 ns) duration.

II. DIAGNOSTICS

The diagnostic tools are: 10-GHz B-dot probe to measure the radiation produced by the rail spark gap (Fig. 2) employed to obtain the Blumlein circuit and the microwave radiation exiting the cavity of the setup given in Fig. 1, Tektronix CT-1 transformer/probe to measure the electrical current in the cavity, Hamamatsu R727 photodiode to record N_2 emission, and 3-GHz Tektronix oscilloscope: Model: TDS 694C to record the data.

B-dot probe made by Advanced Engineering Manufacturing Solutions, Albuquerque, NM 87123, USA, was calibrated in the TEM cell. For a frequency of 1.08 GHz, the amplitude of the signal of 1 V corresponds to the electric fields of 3.07 kV/cm. The amplitude of the signal is linearly proportional to the frequencies in the range from 1 to 10 GHz.

Tektronix CT-1 probe measures the magnetic fields in the cavity in the RF and the microwave domain. The amplitude of signal by the CT-1 probe depends on the orientation and on the position of the probe. The probe is observing only the limited space in the cavity.

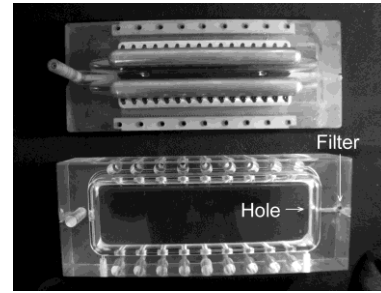


Fig. 2. Top base of the rail spark gap designed to conduct the current up to 500 kA from the capacitor bank charged to the voltage up to 100 kV. Outside dimensions of the base are 38.1 cm times 15.5 cm. The base has two brass electrodes, and the trigger (knife edge) electrode placed in the middle. The diameter of each brass electrode is 3.175-cm diameter and is 33 cm long. Bottom—Plexiglas cover of the rail spark gap. The hole of 6.25 mm was drilled in the Plexiglas cover and the “O” ring, and 337-nm bandpass filter was placed on the top of the hole. The hole is in line with the midsection space between the two main brass electrodes.

Tektronix CT-1 current probe was used earlier in the laboratory to measure the features of “square”-shaped pulses with subnanosecond rise time and the pulse duration of up to 80 ns. This probe can be used instead of the E -field capacitive probe.

Tektronix CT-1 probe records also the radiations coming from the excited molecules and atoms, because these radiations are considered to be the electromagnetic waves that can be described by the electric and the magnetic fields.

Using Rogowski coils made by Pearson Electronics Inc., Model 110, the current supplied by nine-stage Marx generator charged at 15 kV/stage was calibrated. The peak value of the current due to the low (~ 9.2 MHz) frequency of component is ~ 4 kA and equals “600 mV.” Hence, “100 mV/div” scale in the current trace corresponds to 667 A. This low (~ 9.2 MHz)-frequency component of the current dictates the overall shape of the oscillatory current waveform.

In front of Hamamatsu R727 photodiode (of rise time of <1 ns), the 337.1-nm bandpass filter was placed. The filter of 11.8-mm diameter was made by Edmund Optics. The full width at half maximum (FWHM) of the filter is 10 nm.

Tektronix 3-GHz oscilloscope has sufficient numbers of sample points to display correctly the signal of 1 GHz, when the signal was viewed with 5 ns/div timescale. When 10 ns/div timescale was used, the envelope of the pulse was somewhat “rough” giving the appearance that the signal was subject to the “amplitude modulation.” When the larger timescale is applied (i.e., 40 ns/div scale), the oscilloscope cannot display correctly 1-GHz signal.

III. FIRST SET OF EXPERIMENTS

The classical method of N_2 laser production was used. A Blumlein circuit was built to create the glow-like discharges between the two parallel electrodes of the rail spark gap (Fig. 2) and to get the N_2 laser emission. The preionization had to be applied to get a uniform glow-like column. An inexpensive ways of producing preionization is to use the “corona plate/wire” placed some distance away from the two parallel electrodes. To understand how the structure operates, kindly note [6], which gives the waveforms of the voltage, current,

and the laser radiation emitted at 337.1 nm, and explain how the circuit operates.

Review of the literature indicates the laser power at 337.1 nm obtained varies from hundreds of kilowatts to over 1 MW, the energy in the pulse greater than 5 mJ, and the average energy efficiency of 0.4%. This value of 0.4% was calculated using the data presented by 12 different studies that have been stated in [4]. In these experiments, the Blumlein circuit was charged in the range from 8 to 20 kV.

With the rail spark gap (Fig. 2) available in the laboratory, the uniform glow-type discharge was created between the two main electrodes of the rail spark gap. A hole of 6.25 mm was drilled on the narrow side of the Plexiglas enclosure and the “O” ring, and 337.1-nm bandpass filter was placed over the hole. The knife-edge electrode of the rail spark gap was connected via 300-pF capacitor together with 100-M Ω resistor to the ground to provide the preionization. The knife-edge electrode was used as the “corona plate/wire.” Slightly better preionization was achieved by replacing the knife-edge electrode with a thin (0.18-mm diameter) wire. In general, it is necessary to optimize the distance between the “corona plate/wire” and the main electrodes to obtain the maximum energy/power of the laser pulse.

Each electrode of the rail spark gap was connected to a strip line of 35-cm length and a width w of 30 cm. Mylar was used to provide the separation s ($=0.4$ mm) between the plates of the strip line. For the relative dielectric constant $\epsilon = 3$, the impedance of the strip line is $=377 \Omega \times s/(w \cdot \epsilon^{1/2}) = 0.29 \Omega$. The “hot” sides of these two strip lines were joined with the inductor of the large value to get the Blumlein circuit arrangement. This arrangement enables the voltage across the main electrodes to be equal to the voltage at which each single strip line was being charged.

The far end of the single strip line was connected to a low-impedance spark gap that was activated by 30-kV trigger pulse. This strip line was further shaped according to the idea employed in [5].

At low (<20 torr) pressure, the glow-like discharges/plasmas between the electrodes has the visual appearance of the semiuniform band connecting the electrodes. Placing B-dot probe 10 cm above the Plexiglas rail spark gap enclosure to view the midsection of 33-cm-long electrodes, the signal and its fast Fourier transform (FFT) plots are obtained (Fig. 3, shot #1). The data show that each shot has unique FFT signature. No two shots out of 20 shots have the same FFT plot. In shot #2, the spark (filamentary) channel was present in the glow-like column. Such channel was observed in some shots. The time when the spark channel has bridged the gap is marked by t_1 . With the partially developed spark channel present in the glow-like band, the brightness of this plasma band becomes less uniform. As the pressure rises, the developing spark channel would bridge the gap earlier in time and the laser emission would decrease and be of small duration (Fig. 3, shot #2). To limit the onset of the spark channel, the strip lines are made of a short transient time/length so that the stored energy can be dissipated in the glow-like column before the time the developing channel could cross the gap between the main electrodes.

The signals shown in Fig. 3 are the interference signals for the laser detector. They are caused by the glow-like column in shot #1 and in shot #2 by the glow-like column and the spark channel. If these interference signals of shot #2 would be occurring in the structure shown in Fig. 1, the microwave radiation would be obtained as discussed in Section IV. To get the nitrogen laser waveforms shown in Fig. 3, frame C, the interference signals have to be suppressed, because Hamamatsu R727 photodiode design is similar to that of the receiving parabolic microwave antenna. Without suppressing the interference, the signal from the photodiode would display both the laser emission and the microwaves. The interference problem can be solved partially by enclosing the experimental setup to be the Faraday cage that has only small opening to enable the laser beam to exit the enclosure. Without having the enclosure and to avoid the interference problems, the laser signals recorded by the photodiode have been viewed with the aid of low (150 MHz)-pass filter. In Fig. 3, frame C, the laser emissions have been recorded with such filter. To limit the error in the shape/rise time of the laser pulse, the laser emissions were studied only at low (10–30 torr) pressure of nitrogen.

IV. SECOND SET OF EXPERIMENTS

The photograph of nine-stage Marx generator and some of its features are given in Figs. 4 and 5, respectively. When the structure of Fig. 1 was placed on the top of the generator, it can be stated that the generator was placed in the Faraday cage. The interference signals from the generator can penetrate the cavity only through the small gap formed between copper ring 2 and copper plate 3 indicated in Fig. 1.

To appreciate how the structure shown in Fig. 1 works, let us first note that when the graphite electrode, 12 is removed and nine-stage Marx generator is energized; the breakdown discharge takes place between copper plate 2 and copper ring 3. The breakdown occurs in millimeter and submillimeter gaps over the dielectric (Plexiglas) substrate. The gap is subject to high (few MV/cm) fields. These discharges are creating the uniform and rapid UV photoionization in the volume of gas placed inside the cylinder, 11 of Fig. 1, as discussed in [7]–[9].

When the graphite electrode is attached, the voltage across many spark channels created on the circumference of the plate 3 has not fallen to fully zero value. The part of the voltage pulse from the generator will traverse between the graphite electrode and the cylinder until it reaches the end of the electrode. The wave will see the open circuit and will reflect back toward the metallic holder, 4. There, we do not have the matching impedance condition and the wave will travel forth and back along the graphite electrode, creating the electron-impact ionization in the space between this electrode and the cylinder. The electric field of the voltage pulse is well below the voltage breakdown potential. The UV preionization provides and maintains the necessary ionization in the gas to carry the current and provides electrical excitation of the molecules. The plasma produced by the UV preionization was also augmented by the applied electric fields via the Townsend multiplication parameters (defined via the parameter related

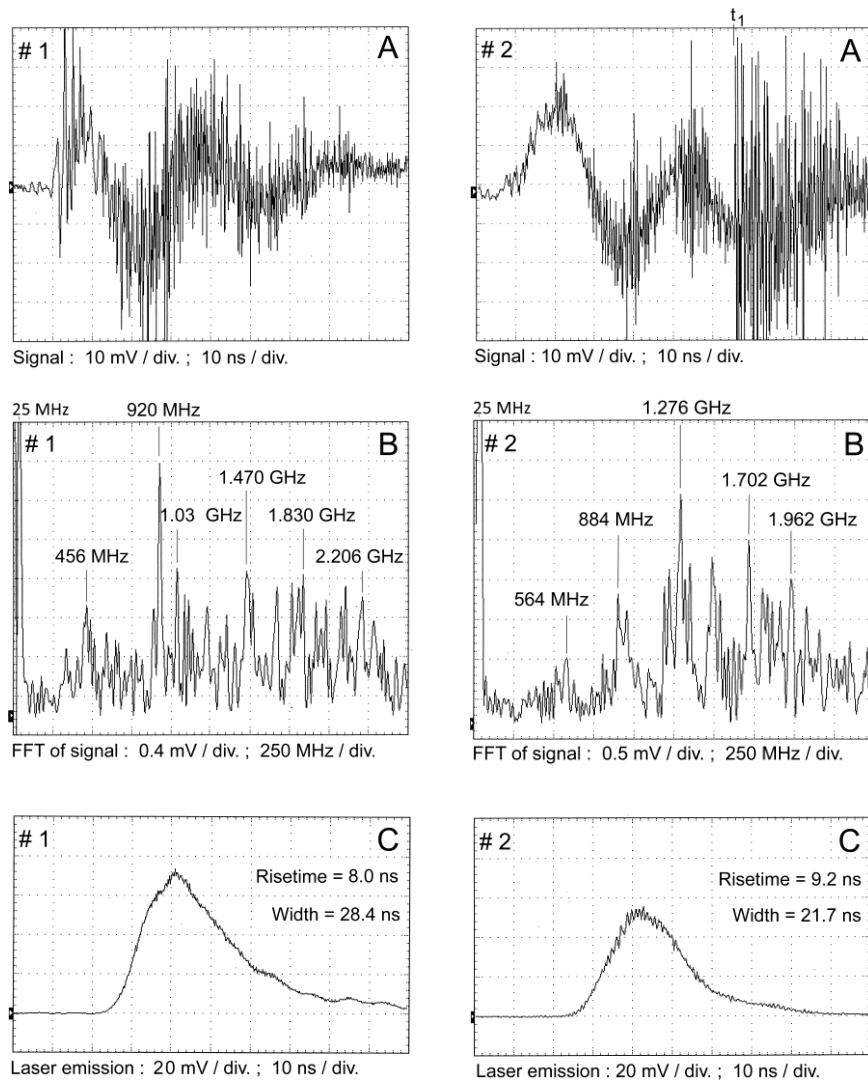


Fig. 3. Two shots recorded at ~ 20 torr pressure of nitrogen. In shot #1, the glow-like column was formed between the two main brass electrodes. In shot #2, the filamentary (spark) channel was also present in the glow-like column. Signals were recorded with 10-GHz B-dot probe. Their FFT plots are given in frame B. Numerous high-frequency signals indicated in frame B are superimposed on the oscillation of the signal with a frequency of 25 MHz. Hamamatsu photodiode R727 together with 337-nm bandpass filter was used to record the laser emission. Blumlein circuit was charged to 12.5 kV. Separation between the two brass electrodes was 8.7 mm.

to the ratio between the electric field and the neutral gas density) together with the parameters related to the high-speed (runaway) electron production.

The amplitude of the electric field on the graphite electrode depends on the value of the charging voltage of the Marx generator, and on the spacing between copper plate 2 and copper ring 3. To get the maximum value of the radiation exiting the cavity, it was learned that the Marx generator has to be charged to the particular (optimum) value. If the charging voltage is a few kilovolts above the optimum value, the voltage across the spark channels will fall causing the decrease of the current flowing between the graphite electrode and the cylinder up to the factor of 2, resulting in the decrease of the ionization and excitation of the constituencies in the gas by the electric field. If the Marx generator is charged to slightly lower voltage in comparison to the optimum value, the trace of the radiation emission will have the steps at the beginning of the emission.

In zero-order approximation, the setup in Fig. 1 could be considered as RLC resonant circuit/cavity that can discriminate/reject the frequencies located away from the resonant frequency on either side of the resonance. This feature is described by the quality factor Q of the resonant cavity. The B-dot probe records the radiation exiting the resonant cavity, and this is dictated by the quality factor Q [9]. As shown in [7], the microwave emission at the resonance can be described in the term of the maser action, which means that the amplification of the microwave in the cavity behaves as a high-gain narrow bandwidth amplifier.

The resonant frequencies exiting the cavity can be considered as coming from the coaxial waveguide. As shown in [7]–[9], the experimental evidence indicates that the TE_{11} mode predominates. The TE_{11} (peak-on axis) has the smallest cutoff frequency value of all the TE modes propagating in the coaxial waveguide. The cutoff wavelength for the

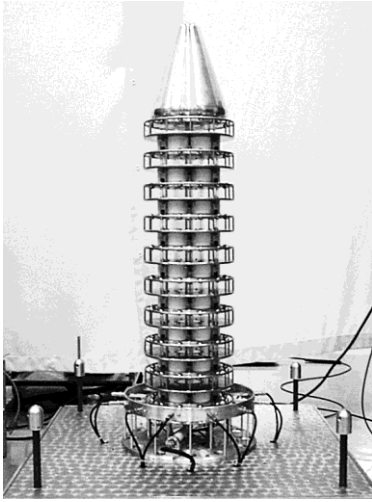


Fig. 4. Interior of nine-stage Marx generator. In the final setup, Plexiglas cylinder is placed between the interior and the metallic tube of 12-inches (30.48-cm) diameter that forms the enclosure of the generator. The specifications of the nine-stage Marx generator are: six capacitors per module for the total of 54 capacitors, 12 spark gaps per stage for the total of 120 spark gaps, each spark gap can be adjusted to few micrometers, the capacitance per stage is 15.6 nF, almost ideal coaxial structure achieved, impedance of the generator is circa 18 Ω , the charging voltage per stage varies from 10 to 25 kV, at 25-kV/stage charge, the stored energy in the system is 44 J, and good reproducibility.

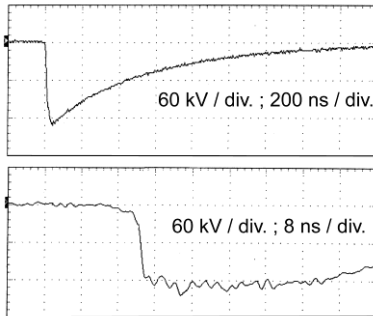


Fig. 5. Output voltage across 300- Ω (18-inches (=45.72-cm) long) resistor. The top trace gives that the width of the double exponential pulse recorded to be ~ 420 ns. The bottom trace gives the rise time to be ~ 2 ns. The generator was charged to 14.7 kV/stage.

TE₁₁ mode is

$$\lambda_c = 1/4 \times 1.873\pi(D + d) \text{ when } D = 3d \quad (1)$$

where D is the diameter of the inner wall of the cylinder and d is the diameter of the graphite electrode of the coaxial waveguide. For $D = 6$ inches (=15.24 cm) and $d = 2$ inches (=5.08 cm) used in Fig. 1, (1) yields $\lambda_c = 29.876$ cm and $f_c = 1.004$ GHz. The experimental data were found to be of the frequency range from 1.060 to 1.083 GHz [9].

Conducting the first set of the experiments and reading the literature, it was learned that the laser emission can be obtained only if the density of the upper-excited $C^3\pi_u$ level is above certain critical threshold. As shown in [4], this means that the curvature of at least one electrode must be of small value, if the Blumein circuit was charged to relatively small (~ 8 to 12 kV) voltage.

For this reason, to get the laser emission in the setup given in Fig. 1, the knife-edge electrode of the rail spark gap was inserted in the cavity. The cross section of the knife-edge electrode is triangle shaped with a base of 1.27 cm and a height of 1.28 cm. This electrode is 33 cm long. The base of this electrode was attached to the inner wall of the cylinder 11. One end of the electrode was placed on step 5 shown in Fig. 1. The electrode was made to be in the parallel position with respect to the graphite electrode. The edge of this electrode was about 3 mm away from the gap formed between the copper ring 2 and the copper plate 3, shown in Fig. 1.

The effect of the knife-edge electrode on the microwave generation is presented in this section, and the effects of this electrode on the laser generation will be given in Section V.

When this electrode is absent, the cavity with the graphite electrode radiates (for example) in argon at 1.080 GHz (Fig. 8, [8]). With the knife-edge electrode present in the cavity, the main frequency exiting the cavity has fallen to 1.052 GHz and the microwave pulse was subject to the amplitude modulation. This modulation varied from shot to shot. The FFT of the microwave signal shown in Fig. 6 gives that this modulation is due to the main frequency lines of the cavity at 1.052 GHz, and the adjacent microwave line at 1.295 GHz.

The current waveform measured with the Tektronix CT-1 probe (Fig. 6) gives the growth and decay of the current component at 1.294 GHz. This component is superimposed on the trace of the current at a frequency of 259 MHz as well on the trace of the low (~ 9.2 MHz)-frequency component. The 259-MHz frequency corresponds to the double transit time for the voltage to travel forth and back along the graphite electrode. The low (~ 9.2 MHz) frequency not noted in Fig. 6 gives the appearance of the oscillatory current waveform.

In Fig. 6, the quality factor Q of the resonant cavity amplifies the low amplitude signal at 1.062 GHz shown in the FFT of the current trace to reach the peak at 1.052 GHz presented in the FFT plot of the signal. The quality factor also suppresses the large amplitude of a frequency of 1.294 GHz shown in the current trace to become the amplitude of smaller value at 1.295 GHz in the FFT plot of the signal.

In general, the interaction between two signals of the same amplitude and of different frequencies f_1 and f_2 is presented [10]

$$\Delta F \times \Delta t = 1 \text{ where } \Delta F = \|f_1 - f_2\| \quad (2)$$

where Δt is the time interval at which the resulting signal has zero value between the two consecutive interactions. Δt keeps repeating in time as long as the signals f_1 and f_2 are applied. In the literature, (2) is referred to describe the coherence effect. Equation (2) can also be applied if the amplitudes of the signal: f_1 and f_2 are not of the same value, and their temporal behavior is different in terms of the decay of amplitude in time.

Using the data presented in Fig. 6, Table I is derived and shows that the experimental difference from the theoretical value is less than 2%.

To learn more about the interaction between these two frequencies, Fig. 7 is obtained. The signal exiting the cavity

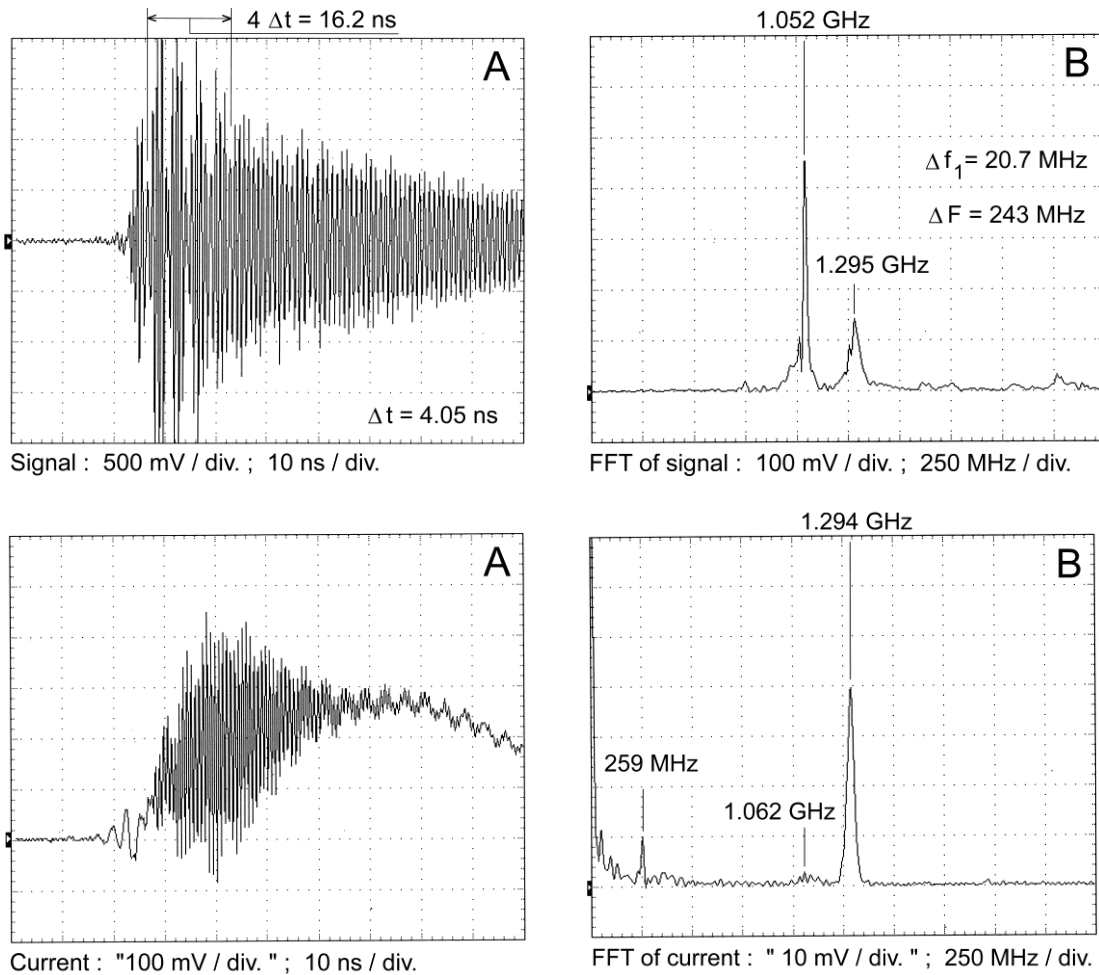


Fig. 6. Experimental data of microwave emission recorded in nitrogen at 150-torr pressure. Signal in frame A was recorded with B-dot probe. Current in frame A was obtained using Tektronix CT-1 current probe. Frames B are the FFT plots of the signal and of the current, respectively. Δf_1 is the FWHM of the line at 1.052 GHz. ΔF is the frequency difference between 1.295 and 1.052 GHz. Knife-edge electrode was present in the cavity. Nine-stage-Marx generator was charged at 12.5 kV/stage.

TABLE I

DATA OF FIG. 6 ARE COMPARED WITH THEORY: $\Delta F \times \Delta t = 1$

	Frequencies (GHz)		ΔF (MHz)	Δt (ns)	$\Delta F \cdot \Delta t$	Difference from $\Delta F \cdot \Delta t = 1$
	Upper	Lower				
Fig. 6	1.295	1.052	243	4.05	0.984	-1.585 %

was viewed by the B-dot probe with the aid of a low (1 GHz)-pass filter. This filter attenuates to some degree the 1.052-GHz signal, but it has suppressed fully the signal at 1.295 GHz. In Fig. 7, shot #1 corresponds to the case, as if the knife-edge electrode would be absent in the resonant cavity. In shot #3, the current waveform has the largest value of the current component at 1.294 GHz that was ever recorded.

V. THIRD SET OF EXPERIMENTS

The knife-edge electrode was introduced in the cavity with the hope of increasing the density of the upper-excited $C^3\pi_u$ level above certain critical threshold to achieve the laser

emission. When the 337.1-nm filter and the photodiode were positioned to view the gap between copper plate 2 and copper ring 3, it was observed from time to time that a small detectable amplitude of the laser emission of circa 12-ns duration was followed by a pause in the emission and low amplitude emissions were recorded to last over 200 ns. In these initial experiments, the nitrogen pressure was 60 torr.

To make sure of having the corona/streamer filament gliding the dielectric (Plexiglas) substrate to be always in line where the filter was located, the experimental setup was modified. The diameter of the copper plate was decreased by 1 cm. The tungsten rod of 1-mm diameter was attached to the metallic holder 4 (Fig. 1). The tungsten rod was positioned to be 2 mm above the copper plate. The gap between the tip of the rod and the copper ring 3 was adjusted to about 1.5 mm.

Under such arrangement, as expected, there would be distribution of the current during the electrical breakdown. Some portion of the current will be conducted by the corona/streamer filament gliding over the dielectric substrate around the circumference of the copper plate. The remaining part of the current will be conducted by the spark breakdown between

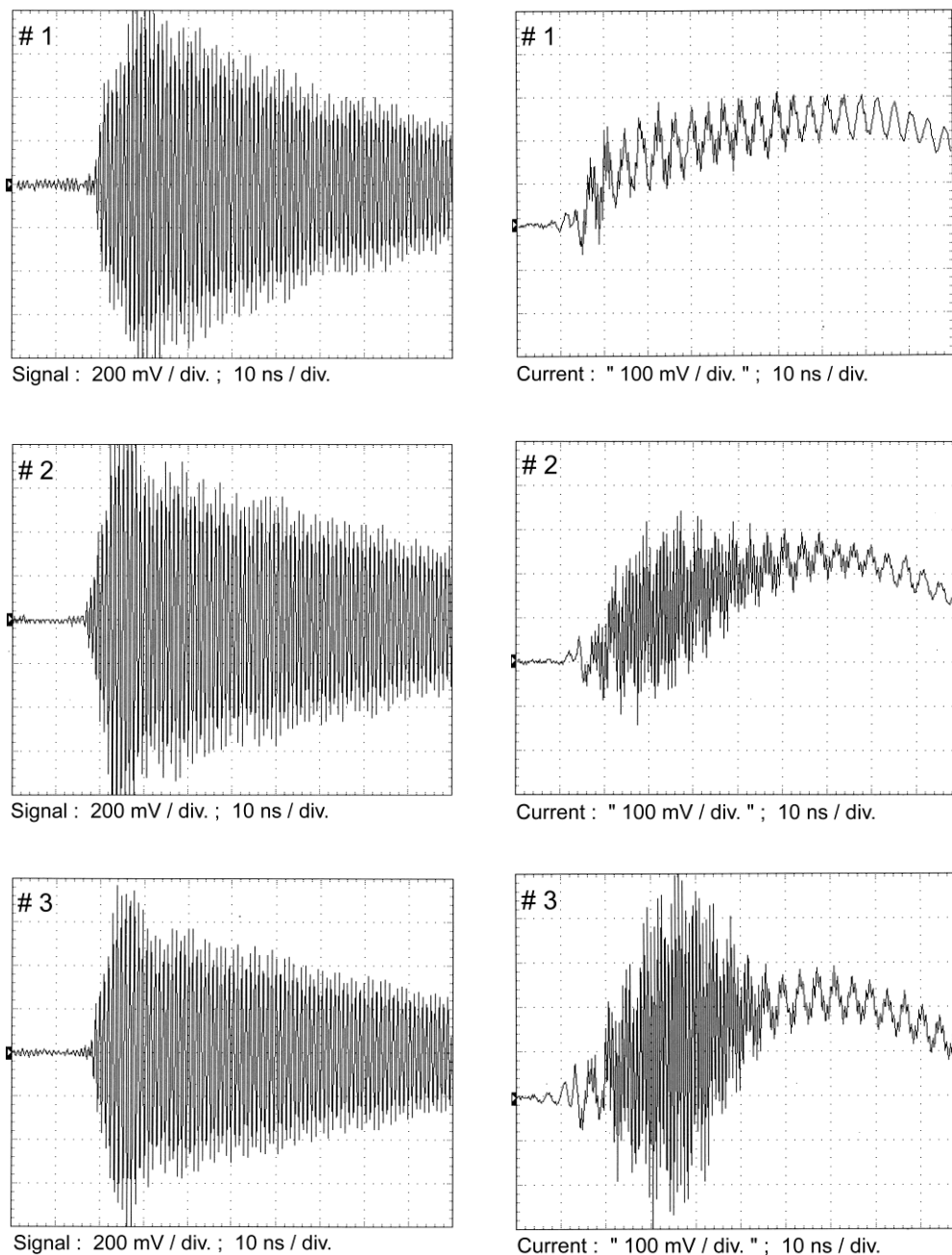


Fig. 7. Three shots of microwave emission at 150-torr pressure are shown in the left, and the corresponding current traces in the right. A frequency of 1.294 GHz presents in the current waveform shown in the right has small amplitude in shot #1 and the very large amplitude in shot #3. Signal and the current were recorded, as in Fig. 6. Knife-edge electrode was present in the cavity. Nine-stage Marx generator was charged to 12.5 kV/stage.

the tip of the rod and the copper ring. By applying higher pressure of nitrogen in the chamber, it was possible to control the amount of the current conducted by the corona/streamer filaments and to ensure that the spark channel would conduct a larger portion of the current.

In Fig. 8, the laser emission at 337.1-nm wavelength was obtained when the nitrogen pressure in the chamber was 150 torr. Fig. 8 also shows that the reproducibility of the laser emission from shot to shot was satisfactory.

Fig. 9 is obtained by changing the nitrogen pressure in the cavity. The data obtained provide some indication how

the laser emission varies versus the current. At the first glance, this dependence appears to be the linear relationship. After the emission reaches the peak value, the exponential decay of the emission was observed in most of the shots recorded. When the pressure in the cavity rises above 250 torr, the decay of the emission was no longer a smooth exponential curve, but rather a modulated curve that follows the oscillations of the current after time t_1 . In Fig. 9, shot #1, t_1 is indicated.

The frequency of the modulation in the decaying portion of the emission is almost of the same value as the frequency

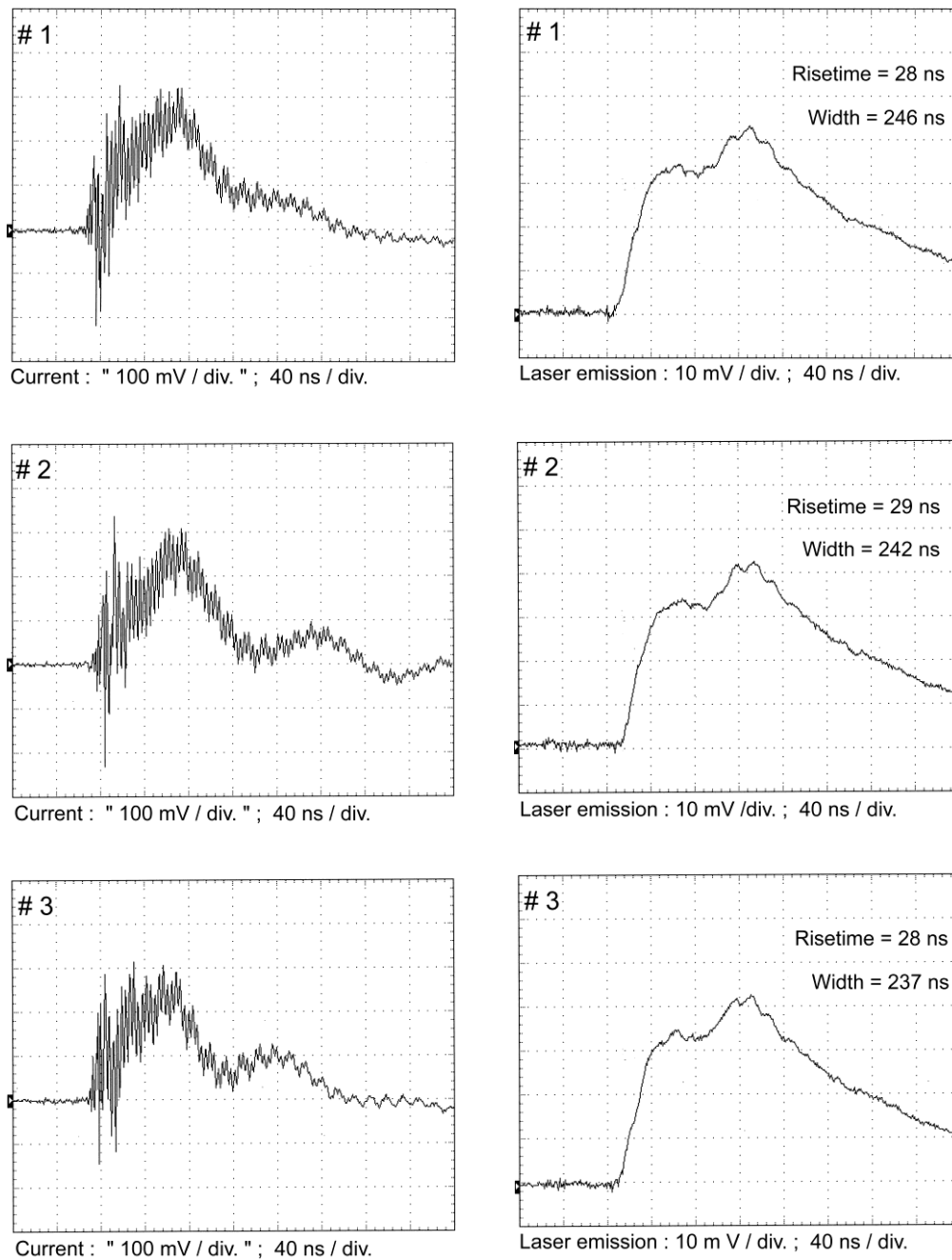


Fig. 8. Three shots of laser emission recorded with the photodiode are shown in the right, and the corresponding current traces in the left. A 150 torr of nitrogen was introduced in the cavity. Knife-edge electrode and tungsten rod were present in the cavity. Current was measured, as in Fig. 6. Nine-stage Marx generator was charged to 15 kV/stage.

in the current waveform; however, the emission has also a strong second harmonics.

When atmospheric air has replaced the nitrogen at 400 torr in the cavity, the emission in air has very similar features. The amplitude and the shape of the pulse remain almost the same. This is a rather surprising and unexpected result.

Please note that the industrial grade nitrogen was used in the experiments, and throughout the measurements of the laser pulse, special care was taken to inhibit the stray light reaching

the photodiode. The radiation at 337 nm was recorded only in all the data presented.

VI. DISCUSSION

To understand the data obtained, it is necessary to learn more about the pumping of N_2 molecules to the upper-excited $C^3\pi_u$ level by the UV radiation and the process of the photoionization.

Photoionization from excited states is the mechanism of gas breakdown by the visible and UV spectrum electromagnetic

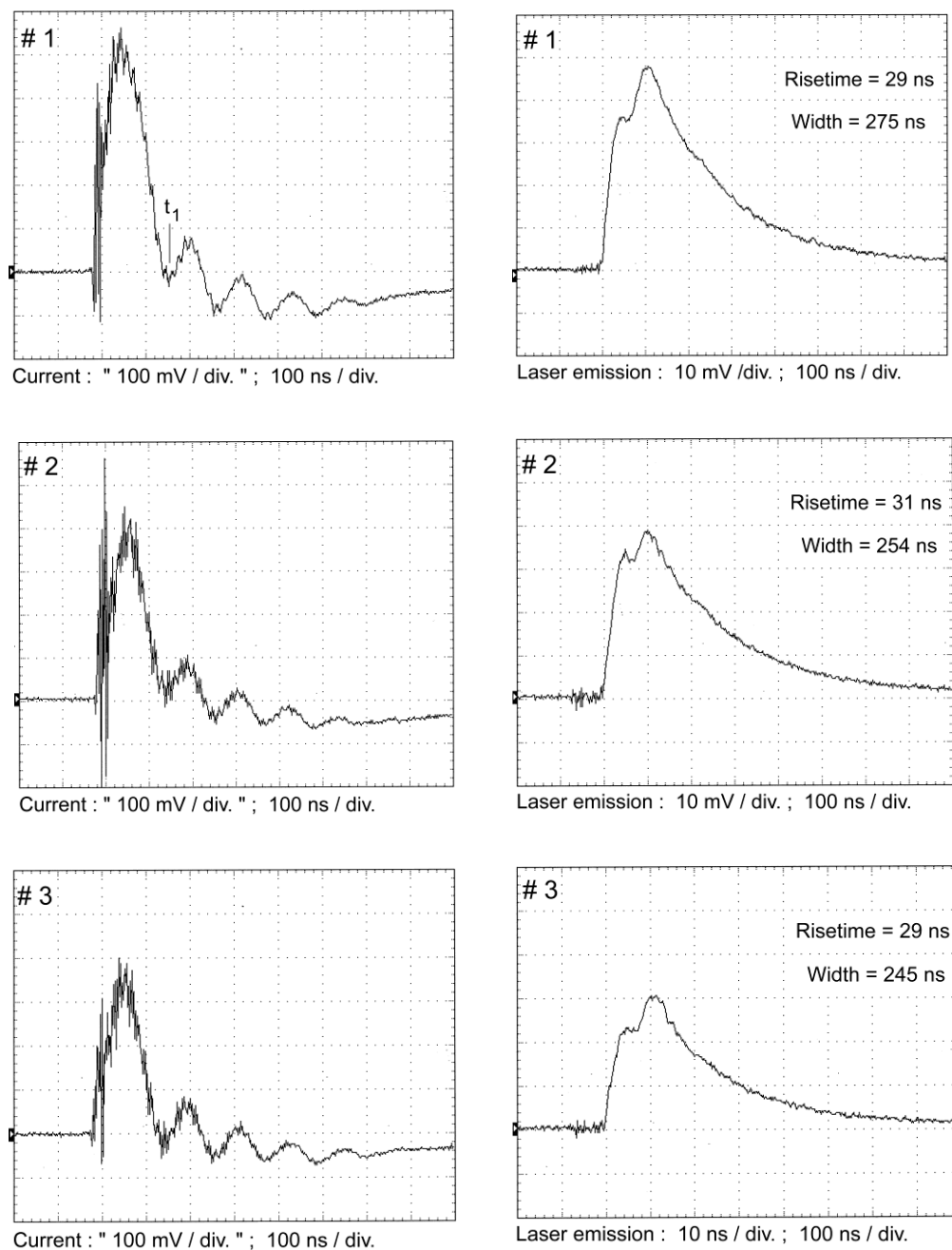


Fig. 9. As in Fig. 8 except the timescale of 100 ns/div was applied. Shot #1 was recoded with 200-torr pressure of nitrogen in the cavity, shot #2 with 150 torr and shot #3 with 100 torr. Knife-edge electrode and tungsten rod were present in the cavity. Nine-stage Marx generator was charged to 15 kV/stage.

waves of high intensity without the benefit of ionization by the external electric field [11], [12]. As a function of the gas density/pressure, the electron densities produced by the UV source have been derived for several gases and gas mixtures by using the microwave interferometry method [12]. Measured at 12 cm from the UV source, the experimental curves show that the electron density in N_2 at 400 torr was $1.7 \times 10^9 \text{ cm}^{-3}$ and about $1 \times 10^{10} \text{ cm}^{-3}$ at 50 torr. The microsecond timescale was used in these measurements. The two tungsten pins adjusted to 2-mm spacing were employed. The condenser charged to 50 kV has supplied 12.5 J to the spark channel discharge to produce the UV source.

The studies reported in [12] have been further elaborated in [13]. Two bands of the hard UV radiation coming from the spark channel were approximately 50 \AA wide centered at 120 nm (energy = 10.34 eV) and the other about 100 \AA wide centered at 175 nm (energy = 7.09 eV).

Coherent lasing actions of N_2 molecules in (plasma) filament in air have been studied in many papers (see [14] and references therein). The N_2 lasing at 337.1 nm was observed in forward and backward directions of the filament created by the powerful laser beam of femtosecond duration. The filament was formed inside the corona discharge. The electric field was applied to produce the corona discharge. The authors

used the term “lasing” to indicate that their N_2 emission yielded the stimulated radiation with the coherence property. When the corona discharge was absent, the amplitude of the N_2 emission was reduced by a factor of more than 2 for the wavelengths at 337 and 357 nm (see [15, Fig. 4(a)]). The timescale of stimulated emission from N_2 molecules is not in the femtosecond regime although the pumping laser pulse is. These are remarkable data, because the femtosecond timescale was used in the study of the excited levels of N_2 over wide range of the N_2 spectrum.

In this paper, the pumping of the upper-excited levels corresponds approximately to the time period from the onset of the current up to the time t_1 shown in Fig. 9, shot #1. This enables to have the laser emission of long (>220 ns) duration.

The main uncertainty to understand the processes above-mentioned is to know how the external electric field influences the production of both the UV preionization, and the upper-excited $C^3\pi_u$ level in N_2 far away from the spark channel. It is obvious that the voltage across the corona streamers and/or the spark channels has the finite value and that this voltage creates the external electrical field across the structure in the setup (Fig. 1), i.e., between the graphite electrode and the cylinder. In [7], the microwave generation in a vicinity of 1 GHz was studied when the setup was not subject to the external electric field (Figs. 3 and 4, [7]). The spark channel was created in another $2\frac{3}{4}$ inches nipple of Fig. 1, and the copper mesh placed at the entrance of the cavity. Afterward, the new data in Figs. 5–7 [7] were obtained when the setup had the electric field. The signal exiting the cavity and the current in the cavity were measured. It was observed that when this external electric field was present, the current flowing in the cavity would rise up to ten times, and the radiation output from the cavity would increase by a factor of (up to) 100 times.

VII. CONCLUSION

In lasers, the laser radiation is produced only at specific frequencies, and the radiation is independent on the size of the cavity. In masers, the radiation is dictated by the size and the quality of the resonant cavity. In the maser case, the system is behaving like a high-gain narrow bandwidth amplifier that has a positive feedback. In the laser case, the system acts as a high-gain broadband amplifier that has a positive feedback.

When the microwave is propagating in the cavity without the knife-edge electrode and occurring in the TE_{11} mode, in this paper, the reproducible results have also been obtained.

To achieve a high level of the microwave production, the strong microwave line in the microwave spectrum is to be chosen and the resonant cavity has to be tuned precisely to match this frequency, as it is the case in the atomic hydrogen maser.

According to [9], the number of excited molecules in air has the powerful radiation line at 7.55 GHz in the microwave domain. This fact means that using (1), the cavity should have the diameter of the cylinder of about 2 cm. Such compact

cavity will have the separation between the graphite rod and the cylinder comparable to the separation between the electrodes used to get the classical N_2 laser energized by the Blumlein circuit. Designing and testing such compact cavity provide the opportunity to obtain simultaneously the laser and the microwave emissions.

It could be interesting to mention some other ideas of the laser production in air, which should be the topic for future research.

Nikola Tesla recorded the puzzling event in his study at Wardenclyffe Tower, Long Island, USA, during 1901–1906 [16]. A bright event to the naked eye at night took place over a large area near the coast line of Long Island and over the sea. It was thought that this bright event had been caused by the electrical discharges triggered by his generator located at Wardenclyffe Tower.

The details of his experiments are unknown and how he achieved the bright event remains not clear. With the diagnostic tools available in the very beginning of the twentieth century, maybe Tesla was not in the position to ascertain the detailed value of the parameters used.

With the current pool of knowledge, the following suggestion can be made. Let us take that the energy comes only from the cumulonimbus clouds. We know that the energy dissipated from the cumulonimbus cloud to the ground in the lightning bolt is up to 500 MJ and carries up to 120 kA and 350 C.

In N_2 laser, the strongest line is at 337.1-nm wavelength in the UV. Among other lines, the next strong line is at 357.6 nm, also UV. This information refers to the second positive system of molecular nitrogen, which is by far the most common. There are also lines in the far-red and infrared from the first positive system, and a visible blue laser line from the molecular nitrogen positive ($1+$) ion.

In the current experiments, the maximum value of the current in the spark channel was circa 4 kA, (stated in Section V) and the intensity of the laser pulse was comparable to the emission produced by the Blumlein circuit. However, the width of the laser pulse obtained is >10 times longer in comparison to the width of the emission recorded with the Blumlein circuit. The spark channel used was circa 1.5 mm long.

On the basis of the evidence above stated, it could be suggested that every short length of the lightning bolt in the processes known as the return strokes will create the nitrogen laser emission, and the visible blue laser line will illuminate a large area causing a bright event as it was in the case of Nikola Tesla experiments.

Tesla’ experiments were done before Albert Einstein first broached the possibility of stimulated emission in 1917 [17]. Einstein postulated that photons prefer to travel together in the same state if one has a large collection of molecules containing a great deal of excess energy. In short, Albert Einstein postulated the laser concept.

Although Nikola Tesla was not in favor of the quantum physics, he has nevertheless provided the support for it ahead of the inception of the laser theory by creating probably the most powerful N_2 laser (=a bright event) in the world at the beginning of the twentieth century.



Fig. 10. Photograph of lightning recorded by Fawn Wood Photography, USA, 2014.

Kindly note Fig. 10, and the opportunity to reexamine the ideas herewith presented in a high-voltage laboratory that has a high-current capabilities and the up-to-date diagnostic sensors.

ACKNOWLEDGMENT

The author would like to thank Dr. D. Villeneuve of the National Research Council of Canada, Ottawa, ON, Canada, for the DET210 high-speed silicon detector made by Thorlabs, MI, USA, used in the initial experiments.

REFERENCES

- [1] B. Hitz, J. J. Ewing, and J. Hecht, *Introduction to Laser Technology*, 3rd ed. Piscataway, NJ, USA: IEEE, 2001.
- [2] H. M. Goldenberg, D. Kleppner, and N. F. Ramsey, "Atomic hydrogen maser," *Phys. Rev. Lett.*, vol. 5, no. 8, pp. 361–363, 1960.
- [3] (Sep. 30, 2017). *Hydrogen Maser*. Accessed: Sep. 30, 2017. [Online]. Available: http://en.wikipedia.org/wiki/Maser#Hydrogen_maser
- [4] A. V. Martinez and V. Aboites, "High-efficiency low-pressure Blumlein nitrogen laser," *IEEE J. Quantum Electron.*, vol. 29, no. 8, pp. 2364–2370, Aug. 1993.
- [5] D. Basting, F. P. Schäfer, and B. Steyer, "A simple, high power nitrogen laser," *Opt.-Electron.*, vol. 4, no. 1, pp. 43–49, Jan. 1972.
- [6] A. Schwab and F. Hollinger, "Compact high-power N₂laser: Circuit theory and design," *IEEE J. Quantum Electron.*, vol. QE-12, no. 3, pp. 183–188, Mar. 1976.

- [7] M. M. Kekez, "Microwave generation in atmospheric air," *IEEE Trans. Plasma Sci.*, vol. 44, no. 10, pp. 2331–2339, Oct. 2016.
- [8] M. M. Kekez, "Microwave generation in air and vacuum," *IEEE Trans. Plasma Sci.*, vol. 45, no. 2, pp. 235–246, Feb. 2017.
- [9] M. M. Kekez, "Method to achieving high-power microwaves in air and argon," *IEEE Trans. Plasma Sci.*, vol. 45, no. 8, pp. 2243–2259, Aug. 2017.
- [10] P. A. Tipler, *Physics*, 2nd ed. New York, NY, USA: Worth Publishers, Nov. 1983, pp. 454–456.
- [11] N. Kopeika and A. Kushelevsky, "The role of excited atoms in UV photopreionization TEA lasers," *IEEE J. Quantum Electron.*, vol. 13, no. 12, pp. 968–972, Dec. 1977.
- [12] H. Seguin, J. Tulip, and D. McKen, "Ultraviolet photoionization in TEA lasers," *IEEE J. Quantum Electron.*, vol. QE-10, no. 3, pp. 311–319, Mar. 1974.
- [13] D. McKen, H. Seguin, and J. Tulip, "Photoionization parameters in the carbon dioxide laser gases," *IEEE J. Quantum Electron.*, vol. QE-12, no. 8, pp. 470–482, Aug. 1976.
- [14] T.-J. Wang *et al.*, "Lasing actions inside a femtosecond laser filament in air," in *Laser Filamentation*(CRM Series in Mathematical Physics), A. D. Bandrauk, Ed. Cham, Switzerland: Springer, 2016, doi: [10.1007/978-3-319-23084-9_5](https://doi.org/10.1007/978-3-319-23084-9_5).
- [15] Y. Wei, Y. Liu, T.-J. Wang, and N. Chen, "Spectroscopic analysis of high electric field enhanced ionization in laser filaments in air for corona guiding," *High Power Laser Sci. Eng.*, vol. 4, p. e8, Mar. 2016.
- [16] M. Cheney and R. Uth, *Tesla: Master of Lightning*. New York, NY, USA: Barnes & Noble, 1999.
- [17] A. Einstein, "Zur Quantentheorie der Strahlung," *Phys. Zeitschrift*, vol. 18, pp. 121–128, 1917. [Online]. Available: <http://adsabs.harvard.edu/abs/1917PhyZ...18..121E>



Mladen M. Kekez was born in 1941. He received the Dipl.-Ing. degree from the University of Belgrade, Belgrade, Serbia, in 1965, and the Ph.D. degree from the University of Liverpool, Liverpool, U.K., in 1968.

From 1971 to 1972 and from 1974 to 2002, he was with the National Research Council of Canada, Ottawa, ON, Canada, where he was involved in the research and development on gas discharges, pulsed-power technology, plasma fusion-related experiments, biophysics, and fluid dynamics. From 1972 to 1974, he was with the University of Alberta, Edmonton, AB, Canada, where he was involved in the research and development on the CO₂ lasers. In 2002, he formed the company High-Energy Frequency Tesla Inc., Ottawa, to continue with research and development. His current research interests include the high-power microwave in air, other gases, and gas mixture.